TPS LINAC Pulsed High-Power RF System Upgrade

The pre-injector of the Taiwan Photon Source (TPS) is a linear accelerator (LINAC)-based system consisting of five major components:

1. Direct current (DC) thermionic electron gun: supports single-bunch mode (SBM, pulse width 1 ns, output charge 2 nC) and multi-bunch mode (MBM, pulse width 200–1000 ns, output charge 5 nC). The maximum repetition rate for both modes is 5 Hz. After acceleration in the electron gun, the beam energy reaches 90 keV.
2. Sub-harmonic pre-buncher: a single-cavity resonator operating at 499.654 MHz that compresses the electron beam pulse width to below 1 ns.
3. Primary buncher: consists of four resonant cavities operating in the 2π/3 mode at 2997.912 MHz (40 °C). It accelerates the electron beam from 90 keV to 300 keV and requires 2 MW of radio-frequency (RF) input power.
4. Final buncher: consists of 16 resonant cavities operating in the 8π/9 mode at 2997.912 MHz (40 °C). It further accelerates the beam from 300 keV to 3 MeV and requires 3.5 MW of RF input power.
5. S-band linear accelerator: includes 156-cell traveling-wave structure operating in the 2π/3 mode at 2997.912 ± 0.03 MHz and maintained at 38–42 ± 0.1 °C. This final stage consists of three S-band accelerator sections (LINAC-ACC1 to ACC3), which raise the beam energy to 150 MeV. Each section requires roughly 16 MW of RF power. **Figure 1** shows the TPS injector system,[1] which was designed and manufactured as a turnkey system by Research Instruments (RI).

Klystron Upgrade

The TPS injector system is powered by three pulsed high-power RF stations. The first RF station (K1) supplies RF power to the Primary Buncher, Final Buncher, and LINAC-ACC1, while the second (K2) and third (K3) stations supply RF power to LINAC-ACC2 and LINAC-ACC3, respectively.

All three stations currently use the Thales TH2100A Klystron (**Fig. 2(a)**).[2] The electron gun in this Klystron has long been associated with a relatively high arcing rate, which is a common cause of failure. Additionally, declining manufacturing quality in recent years has shortened operational lifetimes, directly affecting the reliability of TPS operations.

To address these issues, a Klystron Upgrade Program was initiated in 2024 to replace the TH2100A with the E37310A Klystron (**Fig. 2(b)**)[3] manufactured by Canon Electron Tubes & Devices (CETD). As summarized in **Table 1**, the E37310A's performance and operating parameters are similar to those of the TH2100A and meet TPS LINAC requirements. Experience from the Taiwan Light Source (TLS) LINAC upgrade shows that the E37310A provides

Table 1: Comparison of the specifications of the Thales TH2100 and CETD E37310A Klystrons.

	Thales TH2100	Canon E37310A
Frequency (MHz)	2998.5 ± 1	2998.5 ± 1
Peak Cathode Voltage (kV)	272	295
Peak Cathode Current (A)	286.2	310
Drive Power (W)	126.7	291
Peak RF Output Power (MW)	35.1	35.6
Pulse Width (duration, 75%) (μs)	6.5	7.5
Pulse Width (duration, RF) (μs)	4.5	4.5
Pulse Transformer Turn Ratio	13	14
Klystron Impedance (Ω)	5.62	4.7

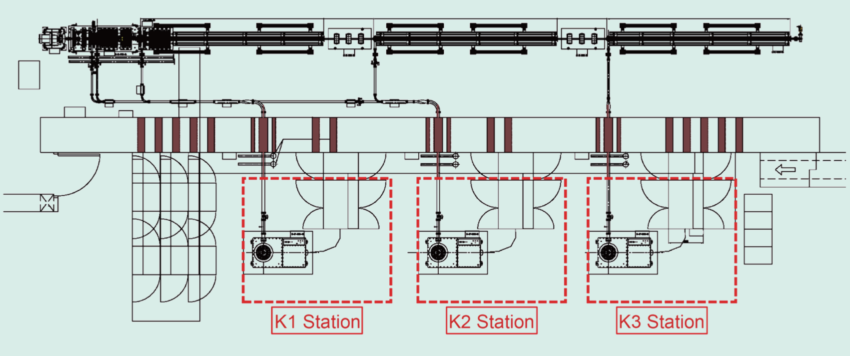

Fig. 1: TPS injector system. [Reproduced from Ref. 1]

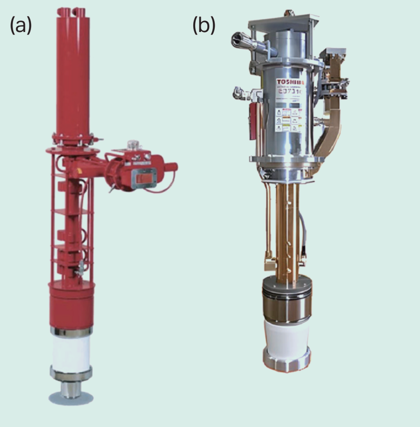

Fig. 2: (a) Thales TH2100 Klystron [Reproduced from Ref. 2] and (b) CETD E37310A Klystron [Reproduced from Ref. 3].

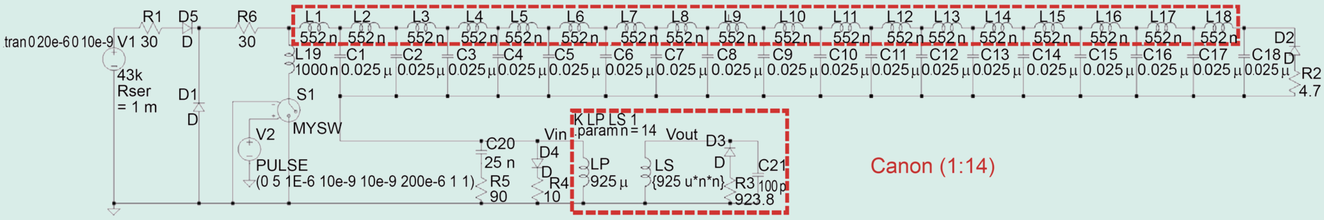

Fig. 3: Circuit model of the newly designed PFN in the pulsed modulator.

excellent operational stability and enhances overall light-source performance. The upgrade also requires modifications to the high-voltage insulating oil tank and the pulsed modulator system to ensure reliable long-term operation.

Klystron Modulator Upgrade

The RI-designed pulsed modulator uses a charging power supply with a maximum output voltage of 45 kV, the upper safety limit for air operation. Under matched conditions, the maximum deliverable primary-side voltage is 22.5 kV. Because different Klystrons require different operating voltages, the transformer turn ratio must be selected carefully, which affects the Klystron oil-tank design.

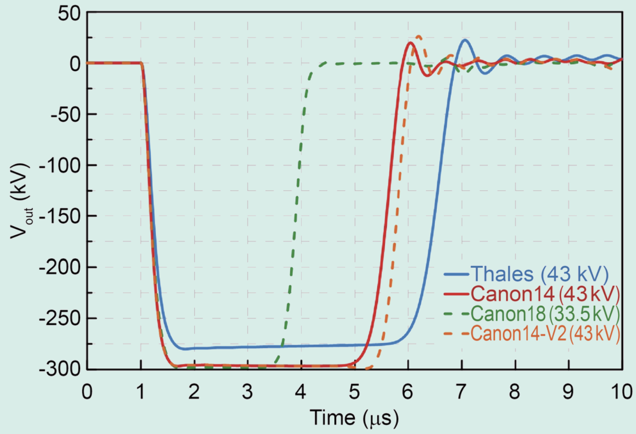

Fig. 4: Circuit-model simulation of the PFN voltage waveforms for the pulsed modulator. Blue: original Thales waveform. Red: Canon PFN with a 1:14 transformer turn ratio. Orange: Canon 1:14 configuration with doubled capacitance in the 18th PFN section. Green: Canon PFN with a 1:18 transformer turn ratio.

The Pulse Forming Network (PFN) consists of 18 sections, each with an inductance of 800 nH and a capacitance of 25 nF, resulting in a calculated PFN impedance of 5.66 Ω (design range: 5–6 Ω). The TH2100A operates at 272 kV and 286.2 A, corresponding to a secondary impedance of 950 Ω. With a 1:13 transformer, the primary impedance is 5.62 Ω.

The E37310A operates at 291 kV and 315 A, corresponding to a secondary impedance of 923.8 Ω. With the same 1:13 transformer, the primary impedance becomes 5.47 Ω; however, reaching the required cathode voltage would require 44.77 kV—too close to the system's maximum rating. A 1:14 transformer reduces the primary impedance to 4.7 Ω and requires only 41.57 kV, which remains within specifications. Considering equipment limits, stray inductances, and practical matching constraints, the 1:14 configuration is selected.

The next step is to carry out PFN redesign and optimization. To meet the operating requirements of the E37310A and obtain a flat, sufficiently wide voltage pulse, PFN simulations and design optimization are performed using LT-Spice (**Fig. 3**). Since the PFN capacitances cannot be easily changed, the inductances are redesigned and reduced from 800 nH to 552 nH to achieve the required impedance.

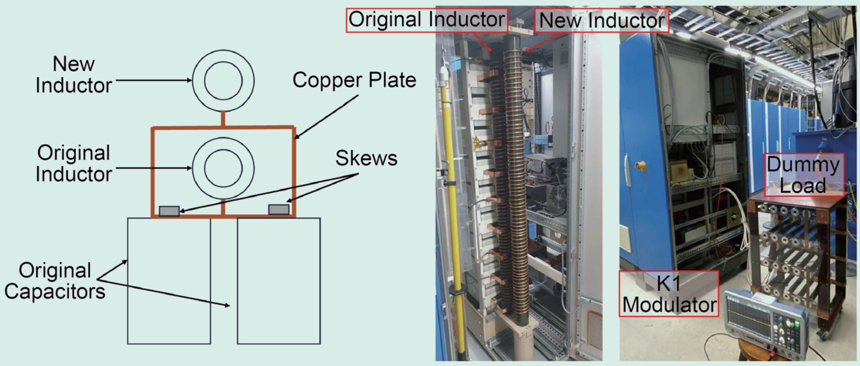

Fig. 5: PFN pulsed modulator: revised configuration diagram and photograph of the completed installation.

Simulation results (**Fig. 4**) show that all turn-ratio configurations produce peak inverse voltages within Klystron specifications. Increasing the transformer ratio from 1:13 to 1:14 shortens the output pulse width by ~1 μs, but overall performance remains acceptable. For comparison, the 1:18 transformer used in TLS reduces pulse width by 2.5 μs, which is unsuitable for TPS.

Doubling the capacitance of the 18th PFN section increases the pulse width by approximately 0.3 μs (**Fig. 4**). A new inductor string is installed in parallel with the original inductors to achieve the required 552 nH. The final PFN configuration and installation are shown in **Fig. 5**.

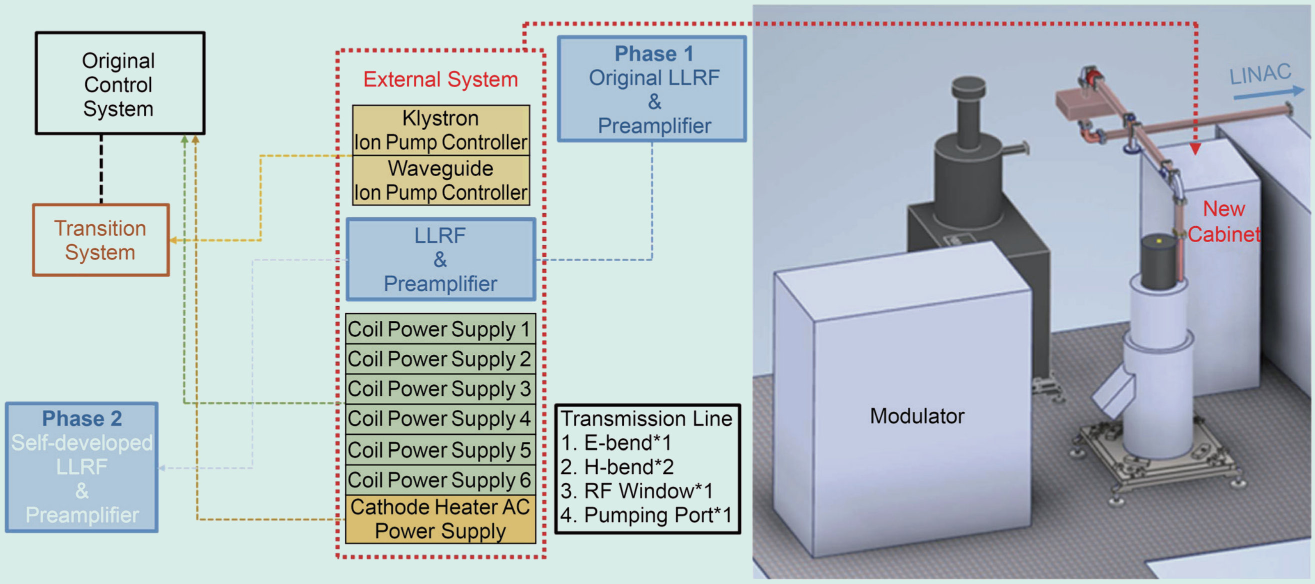

Fig. 6: Revised K1 Station configuration.

Operation Experience with the New Klystron and Modulator

Phase I of the TPS LINAC Klystron upgrade was completed in October 2025. The K1 Station Klystron was replaced with an E37310A, and the pulsed modulator was upgraded. **Figure 6** shows the new system configuration, and **Fig. 7** provides photographs of the installation.

Fig. 7: Installed K1 Station (left) and RF transmission line (right).

Under the test conditions—a pulse repetition rate of 3 Hz, RF pulse width of 4.5 μs, Klystron cathode voltage of 281 kV, and cathode current of 305 A—the E37310A produced 36 MW of RF output power (**Fig. 8**), confirming correct impedance matching and stable modulator performance.

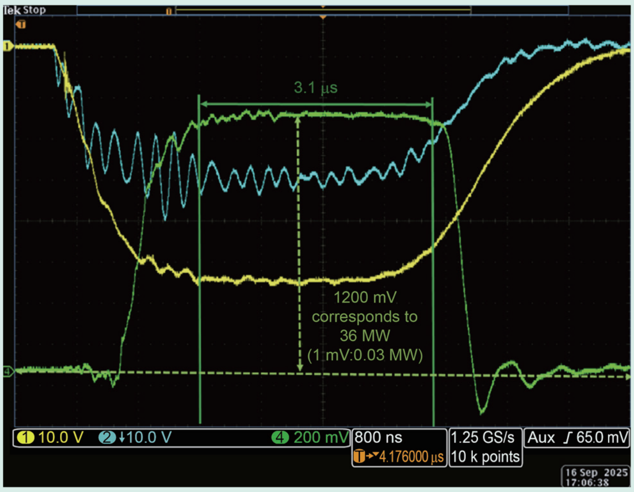

Fig. 8: E37310A Klystron cathode voltage (yellow), cathode current (blue), and RF output power (green).

Conclusion

The redesigned pulsed modulator system achieves a 3.1 μs voltage flat-top, closely matching simulation results and meeting TPS operational requirements. This upgrade also strengthens NSRRC's in-house capability for pulsed modulator development and enhances the potential for future system development.

Extensive testing of TH2100A and E37310A has established standardized operating and maintenance procedures, enhancing safety, efficiency, and reliability. The upgraded RF system has been in routine operation for two months with stable performance.

Phase II of the upgrade will begin in January 2026 and will focus on the K2 Station, further enhancing the stability and reliability of the TPS LINAC. (Reported by Wei-Yuan Chiang)

References

1. TPS 150 MeV Linac Documentation (2008).
2. A. Beunas, THALES RF Sources for Accelerator Recent Developments, July 1 (2019). https://indico.cern.ch/event/804400/contributions/3485023/attachments/1873472/3084546/THALES_presentation_CompactLight_Midterm__Helsinki_2019-rev2-16-9.pdf
3. Microwave Tubes Product Catalog, April (2025). https://etd.canon/en/download/files/microwave_tube_catalog_EN.pdf

Application of AI Intelligent Control in Utility Systems

At the Taiwan Photon Source (TPS), ongoing research is exploring artificial intelligence (AI)-driven methods to enhance energy efficiency across utility systems. Cooling systems account for nearly half of the facility's total energy consumption, making their proper operation essential for reducing overall power demand, as shown in **Fig. 1**. The use of AI for optimizing utility systems is rapidly expanding, particularly in large facilities where chilled water systems and cooling towers represent a significant portion of energy use. AI-based control strategies offer predictive, adaptive, and real-time optimization, providing distinct advantages over traditional rule-based approaches. Studies have demonstrated that AI-driven control can substantially improve both energy efficiency and system reliability in central cooling applications.[1] In critical environments, such as hospitals, advanced optimization methods have achieved considerable energy savings by dynamically adjusting operating parameters in response to changing load and ambient conditions.[2] In complex systems with heterogeneous parallel chillers, neural network-based frameworks have coordinated chiller and cooling tower operations to minimize overall energy use.[3] Building on these advancements, this study applies an AI-based analytical framework to the utility systems at TPS.[4] The model evaluates the impact of ambient wet bulb temperature on overall system behavior and identifies optimal control actions such as adjusting temperature setpoints, pump flow rates, equipment scheduling, and frequency control that can reduce energy consumption while maintaining stable operation. By integrating data-driven modeling with actual operating records, the analysis quantifies potential energy savings and demonstrates that AI-optimized strategies can enhance both efficiency and operational reliability under real-world conditions.

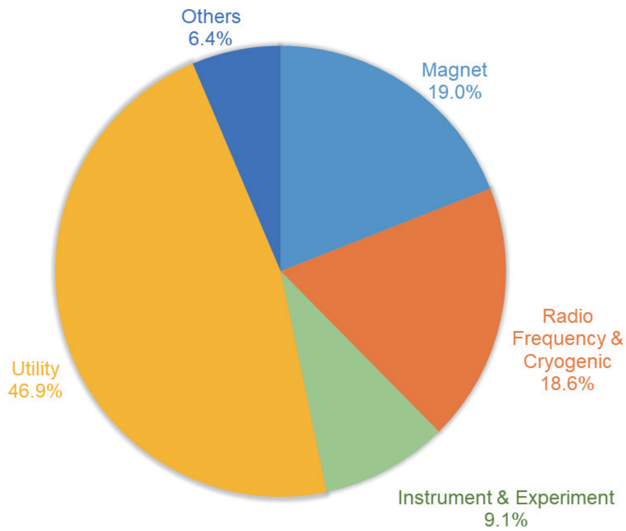

Fig. 1: Power consumption distribution among TPS subsystems.

Model Creation of Cooling Towers and Chilled Water Systems

To improve the efficiency of large-scale cooling and chilled water systems, a data-driven modeling framework was developed. Real-time monitoring was applied to all major equipment, including chilled water pumps, cooling water pumps, chillers, and cooling towers, to collect high-resolution operational data. Each unit operated with independent parameters, enabling flexible and optimal control under varying loads. Power sensors were regularly inspected and calibrated to ensure data accuracy and reliability. System efficiency was assessed by analyzing different operating settings across diverse environmental and load conditions. Machine learning techniques were used to capture nonlinear relationships between equipment behavior and external factors, such as weather and seasonal variations, supporting energy forecasting and early fault detection. Iterative testing and hyperparameter tuning further improved model robustness and predictive accuracy.

Among modeling approaches, recurrent neural networks (RNNs) were selected for their ability to process sequential sensor data, as they retain temporal context unavailable to feedforward networks. To improve long-term dependency learning, the